

Charge-Transfer Dynamics in Azobenzene Alkanethiolate Self-Assembled Monolayers on Gold

Cornelius Gahl, Roland Schmidt, Daniel Brete, Stephanie Paarmann, Martin
Weinelt

Fachbereich Physik, Freie Universität Berlin, Arnimallee 14, 14195 Berlin, Germany

Abstract

We have studied the charge transfer dynamics in azobenzene-functionalized alkanethiolate self-assembled monolayers. We compare the core-hole clock technique, *i.e.*, resonant *vs.* non-resonant contributions in the azobenzene autoionization of the $C1s-\pi^*$ core exciton, with the lifetime of a molecular resonance determined by two-photon photoemission spectroscopy using femtosecond laser pulses. Both techniques yield comparable charge-transfer times of 80 ± 20 fs for a linker consisting of three CH_2 groups and one oxygen unit. Thus the quenching of the excitation is about one order of magnitude faster than the time required for the *trans* to *cis* isomerization of the azobenzene photoswitch in solution.

Keywords: self-assembled monolayers, charge transfer, core-hole clock, time-resolved photoemission, molecular switches

2010 MSC: 00-01, 99-00

1. Introduction

Photochromic molecules can serve as reproducible building blocks to optically manipulate and control surface and interface properties on the nanoscale [1, 2]. This opens up interesting fields of application such as the operation of molecular actuators and motors, the development of switchable sensors, or the
5 biasing of charge transport across organic devices [3, 4]. Given the impressive

*Corresponding authors: C. Gahl (c.gahl@fu-berlin.de) and M. Weinelt (weinelt@physik.fu-berlin.de)

examples in biology and the large variety of photochromic molecules in solution, a major challenge is to ensure that the molecular switch maintains its functionality when adsorbed on a surface. On the one hand excitations in the substrate can lead to a quenching of the photoexcited state [5]. Therefore the coupling between molecular switch and substrate excitations must be controlled by spacer groups. On the other hand, steric and excitonic interactions among the chromophores in the adsorbate layer can impede efficient switching [6]. The latter problem can be overcome introducing large platforms or lateral spacers [5, 7, 8].

One of the best investigated molecular linker systems comprises the class of alkanethiols, which form self-assembled monolayers (SAMs) on gold substrates [9, 10, 11, 12]. We employ SAMs to form well-ordered surface ensembles of azobenzene-functionalized molecules as well as to effectively decouple the photoswitch from the substrate. As sketched in Fig. 1 the azobenzene entity is coupled to the alkane chain *via* an oxygen bridge in para-position. The alkyl chain binds with the sulphur head group to the Au(111) surface and the molecules orient preferentially upright in the SAM with an angle of $\sim 30^\circ$ with respect to the surface normal [6]. Different rest groups ($R = H, CN, CF_3$) were used as markers for X-ray photoelectron and near-edge X-ray absorption spectroscopy (XPS and NEXAFS) studies [6, 13, 14]. In the following the molecules are referred to as R-Az n , where n denotes the number of CH_2 units of the alkyl linker.

In the present article azobenzene-functionalized SAMs on gold serve as a model platform to study the coupling between photoswitch and substrate. We compare two experimental methods, resonant photoemission and time-resolved two-photon photoemission, which both allow for determining the charge-transfer (CT) time of electrons excited to the lowest unoccupied molecular orbitals (LUMO+n) into the substrate. Independent of the alkyl spacer length ($n = 3, 6, 10$) the autoionization spectra of the azobenzene moiety are dominated by spectator and participator decay channels. Following the decay of the C1s to LUMO+1,2 resonances the dominant participator-decay line shows a lower in-

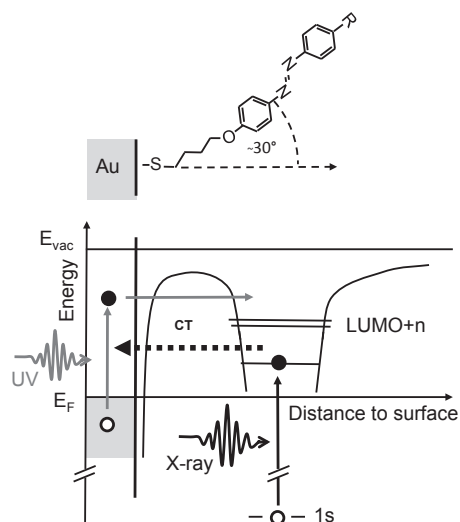


Figure 1: Alkanethiols bind with the sulphur headgroup to the Au(111) surface and orient preferentially upright in a self-assembled monolayer (SAM). Thereby the alkyl chain shapes a tunnel barrier, which allows for decoupling the azobenzene endgroup from the Au metal. The unoccupied molecular orbital (LUMO+n) is populated either indirectly by electrons optically excited in the gold substrate employing ultraviolet (UV) laser pulses or by resonant intramolecular excitation of a 1s core electron using X-rays. The charge-transfer (CT) time is determined by probing the excited state with a second laser pulse in a time-resolved photoemission experiment or by disentangling resonant autoionization from non-resonant Auger contributions in the core-hole decay.

tensity for shorter chain length. Applying the core-hole clock we obtain for the CF₃-Az3 SAM a charge-transfer time of 73 ± 20 fs.

40 The 2PPE spectra of H-Az3 show a negative ion resonance at $E - E_F = 3.6$ eV, which we attribute to a LUMO+n of the azobenzene chromophore. The resonance has a lifetime of 80 ± 20 fs in good agreement with the result from the core-hole-clock technique. While the charge-transfer time is compatible with a tunnel barrier of thickness $n = 4$ [15, 16], it seems unaffected by the resonance
45 position.

2. Experimental

The various R-Azn compounds were synthesized and purified as described elsewhere [13, 17]. Their purity has been verified by ultrahigh-performance liquid chromatography. As substrates we used 200 nm thick gold films on mica
50 (Georg Albert PVD), which exhibit large Au(111) terraces. SAMs were prepared by immersing the substrate into 10^{-4} molar ethanolic solution for 24 hours. Afterwards the samples were copiously rinsed with pure ethanol, blown dry with argon, mounted on the sample holder and directly transferred into the ultrahigh-vacuum chambers (base pressure $\leq 2 \cdot 10^{-10}$ mbar). The preparation
55 procedure was routinely controlled by XPS [13, 14].

We used two separate experimental setups for resonant and time-resolved photoemission. Both apparatus were equipped with comparable load locks and sample holders for sample transfer and cooling. To reduce X-ray beam-damage experiments were performed at a sample temperature of ~ 120 K [18, 19] and
60 the X-ray exposure was minimized by scanning the sample and using a fast beam shutter.

Resonant photoemission experiments were performed at the undulator beam-line U41 PGM-1 of the synchrotron facility BESSY II, Helmholtz-Zentrum Berlin. We used a hemispherical analyzer (Omicron, EA125) equipped with
65 5 channeltrons. The total energy resolution of the measurements was 0.2 eV as established by the width of the S2p XPS line and the Fermi level of the

clean gold substrate. Measurements were performed in grazing incidence with an angle of 15° between X-ray beam and surface plane. The analyzer chamber is rotatable around the beam axis. In this way the polarization of the incoming X-ray beam was set parallel to the surface plane and the angle of electron
70 detection normal to the surface. This measurement geometry optimizes the ratio between the autoionization signal and the photoemission background [20]. The photon energies and the binding energy scale are referenced to the binding energy of the Au $4f_{7/2}$ core level of 83.95 eV [21].

75 The laser system for 2PPE spectroscopy consists of two optical parametric amplifiers, both pumped by a Ti:Sapphire amplifier system running at a repetition rate of 300 kHz (Coherent, RegA). In this way independently tunable visible and ultraviolet (UV) light pulses are generated with a duration of ~ 50 fs and pulse energies of ~ 25 nJ and 3 nJ, respectively. A translation stage is used to
80 adjust the delay of the visible pulse. Both beams impinge nearly collinearly on the sample in the horizontal plane, which forms an angle of 45° to the surface normal. Emission angle and kinetic energy of the photoemitted electrons are measured using a hemispherical electron analyzer (SPECS, Phoibos 100) equipped with a two-dimensional view-type detector.

85 **3. Results and Discussion**

3.1. The core-hole clock

One means of studying the charge transfer-time between adsorbate and substrate is the so-called core-hole clock (see, *e.g.* [22] and refs. therein). This method was pioneered by the groups of Dietrich Menzel in Munich and Nils
90 Mårtensson in Uppsala initially investigating rare gas layers physisorbed on metal surfaces [23, 24]. The method's keynote is illustrated in Fig. 2. A core-to-valence excitation starts the core-hole clock, which stops on the time scale of the core-hole lifetime τ_{Γ} . If charge transfer between the excited valence level and the substrate occurs prior to the core-hole decay, one records an ordinary, *i.e.*,
95 non-resonant Auger spectrum. In contrast, if the excited electron stays on the

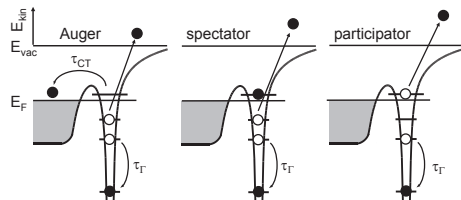


Figure 2: Schematics of the core-hole decay. After resonant excitation of a core-exciton, the charge-transfer time τ_{CT} is deduced by reference to the core-hole lifetime τ_T comparing the intensities of non-resonant (Auger) and resonant (spectator, participator) decay channels: $\tau_{CT}/\tau_T = (I_{Auger} + I_{spectator} + I_{participator})/I_{Auger}$.

adsorbate it may either participate in the autoionization or additionally screen the core-hole decay. This results in either an enhancement of photoemission lines (participator decay) or a screening shift of the Auger decay spectrum to higher kinetic energies (spectator shift). Assuming exponential decay, the charge transfer time τ_{CT} can be deduced from the intensities of non-resonant I_{Auger} and resonant $I_{participator} + I_{spectator}$ Auger channels $\tau_{CT}/\tau_T = (I_{res} + I_{Auger})/I_{Auger}$ [25, 26]. Given core-hole lifetimes of 6.6 and 5.4 fs for the carbon and nitrogen $1s$ -levels [27, 28], charge-transfer times ranging from sub-fs to about 100 fs can be determined. For the light elements the X-ray emission yield is below 1 % and can be neglected. A major advantage of the core-hole-clock technique is its sub-monolayer sensitivity, which results from the pronounced cross section of resonant core-to-valence transitions. A challenge for larger molecules is the increasing number of Auger decay channels. In combination with vibrational excitations, they lead to complex decay spectra, which are hard to decompose.

3.2. Core-ionized vs. core-excitonic state of azobenzene

In the core-ionized state a core hole in the azobenzene endgroup will be screened by polarization of the SAM and the gold substrate. In the core-excitonic state the binding energy of the resonantly excited occupied molecular level is increased mainly by the Coulomb interaction with the core hole. To observe charge transfer between adsorbate and substrate it is a prerequisite that

the energy of the excited molecular level stays above the Fermi level in the core-excitonic state. In other words, the energy of the NEXAFS resonance has to exceed the XP binding-energy of the core electron, which refers to E_F . In the azobenzene moiety this becomes element-specific. Figures 3a and b compare
120 the XP and NEXAFS spectra of the chromophore's N1s and C1s core-levels (top and bottom panels) for SAMs with alkyl chain-lengths of $n = 3, 6$ and 10, respectively. Note that on the common energy scale the abscissae of the XP spectra are reverted so that shake-up excitations are observed on the right of the main line. Given the preferentially upright geometry of the molecules in all
125 SAMs and the inelastic mean-free-path of the photoelectrons [29, 30] the C1s XP signal is dominated by the azobenzene chromophore with minor contributions from the alkyl chain.

As evident from Figs. 3a and b the core-hole binding-energies, *i.e.*, the core-ionized XP final states depend on the alkyl chain length. Both N1s and C1s peak
130 maxima shift by ~ 400 meV to higher binding energy with increasing number of CH₂ units. This shift is attributed to a final state effect as the initial state of the chromophore is comparable for all chain lengths. Image-charge screening of the core hole becomes less efficient for larger distance to the metal substrate. Therefore the binding energy increases for longer spacer length. A similar effect
135 has already been observed in the C1s XP spectra of alkanethiolate SAMs [31] and for the N1s XP line of a cyano end group [16].

In contrast to the varying XP binding energies the π^* -resonances stay at constant energy independent of the alkyl chain-length. Screening of the core hole is dominated by the interaction with the electron in the unoccupied molecular
140 orbital forming the core exciton. The resonance at the nitrogen absorption edge at 398.3 eV is assigned to the azobenzene N1s to π^* LUMO transition. Its energy is lower than the N1s XP peak maximum of CF₃-Az3 at 399.4 eV. As a consequence the core exciton can solely decay *via* autoionization but not *via* transfer of the excited electron into unoccupied states of the substrate.
145 The significant broadening of the π^* -resonance beyond the natural linewidth of 100 meV is therefore attributed to vibrational excitations.

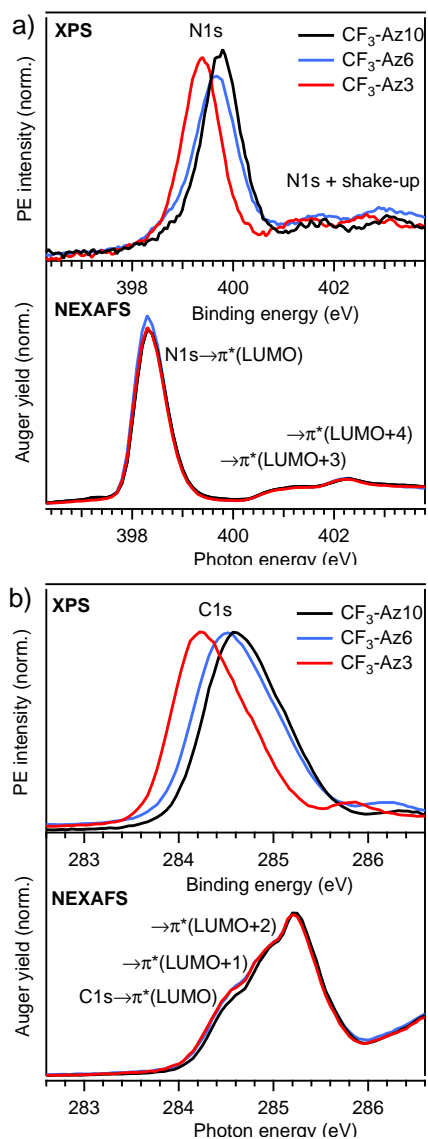


Figure 3: Comparison of core-ionized and core-excited states in XP and NEXAFS spectroscopy for CF₃-Az_n SAMs with alkyl chain-lengths $n = 3, 6$ and 10 at a) the nitrogen and b) the carbon $1s$ edge. XP and NEXAFS spectra are plotted on a common energy scale referring to the $1s$ binding energy and the photon energy, respectively. The XP spectra shift to higher binding energy with increasing chain length reflecting the reduced image-charge screening of the XP final state by the substrate. At the N1s edge the π^* -resonance is lower in energy than the XP core level. Thus the LUMO is pulled below the Fermi energy in the core-excited state and charge transfer from adsorbate to substrate can not occur. In contrast at the C1s edge charge transfer is possible out of the energetically higher LUMO+1 and LUMO+2 resonances.

The situation is different at the C1s absorption edge. The first absorption line shows a multiple peak structure, which reflects contributions from the LUMO as well as the LUMO+1 and LUMO+2. A contour plot of the unoccupied orbitals can be found in Fig. 6 of Ref. [13]. The energy of the resonance maximum at 285.25 eV is clearly above the XP peak position at 284.2 eV ($n = 3$). Therefore charge transfer between the azobenzene chromophore and the gold substrate can occur after resonant excitation of the C1s level.

3.3. Charge-transfer time

To study the charge-transfer time we concentrate in the following on the decay spectra after C1s excitation. Figure 4a shows three photoemission spectra of CF₃-Az3 recorded for photon energies below, at, and above the C1s resonance maximum. The photoemission spectra have been normalized to the gold valence band intensity and are plotted on a kinetic energy scale.

The spectrum recorded below the π^* -resonance at $h\nu = 275.0$ eV is dominated by photoemission from the gold $6sp$ and $5d$ valence bands, which extend over a range of ~ 11 eV below E_F [32]. In addition there are minor contributions from the valence orbitals of the SAM and the C1s XP line at 262 eV kinetic energy ionized by the second harmonic of the undulator ($2h\nu = 550.0$ eV).

The spectrum recorded at a photon energy of 312.0 eV above the ionization threshold is representative for non-resonant Auger decay. The multitude of azobenzene valence orbitals involved in the KVV decay of the C1s core hole give rise to a weakly structured 30-eV wide Auger peak centered at a kinetic energy of 260.0 eV.

Tuning the photon energy to the resonance maximum at 285.25 eV we resonantly excite the close lying LUMO+2 and LUMO+3, which extend over the outer and inner phenyl ring of the azobenzene chromophore, respectively. These core-excited states predominantly decay *via* resonant photoemission. The center of mass of the autoionization spectrum is at 262.0 eV kinetic energy and the spectrum exhibits a more pronounced fine structure as compared to the non-resonant Auger decay. The higher kinetic energy is attributed to a spectator

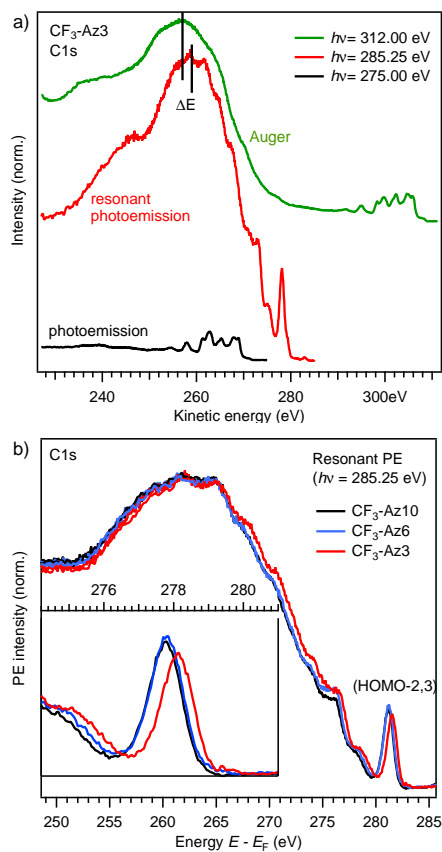


Figure 4: a) Photoemission spectra of a $\text{CF}_3\text{-Az3}$ SAM recorded with photon energies below ($h\nu = 275.0$ eV), at ($h\nu = 285.25$ eV), and above ($h\nu = 302.0$ eV) the maximum of the C1s to π^* LUMO+1,2 transitions (*cf.* Fig 3b). Spectra have been normalized to equal intensity of the Ausp band 1 eV below E_F . The vertical bars indicate the spectator shift. The HOMO-2,3 participator line is strongly enhanced at resonance. b) Comparison of resonant photoemission spectra of $\text{CF}_3\text{-Az}n$ for alkyl chain length of $n = 3, 6$ and 10 . All spectra have been recorded at a photon energy of 285.25 eV and are normalized to equal intensity after subtracting the non-resonant photoemission background. The shift of the spectra is a final state effect attributed to distinct polarization screening. As highlighted in the inset the HOMO-2,3 participator decay line has a $9 \pm 2\%$ lower intensity for the shortest alkyl chain length $n = 3$ as compared to $n = 6$ and 10 .

shift of 2.0 ± 0.2 eV and the fine structure to additional participator decay lines. The comparable width of the Auger and autoionization spectra indicates that there exist only weak contributions of non-resonant Auger decay at resonance. In other words, the charge transfer between adsorbate and substrate must be slow compared to the core-hole lifetime. The most prominent spectator line of the autoionization spectrum is observed at a kinetic energy of 278.15 eV, which corresponds to a binding energy of $E - E_F = 2.7$ eV. It is attributed to the nearly degenerate HOMO-2 and HOMO-3 of the azobenzene moiety, which extend over the inner and outer phenyl ring, respectively. The HOMO is the lone-pair orbital of the azo-bridge and thus localized at the nitrogen atoms. It is therefore not enhanced in resonant photoemission at the carbon edge. Given the small spectator shift in C1s autoionization it is very difficult to decompose the decay spectra in resonant and non-resonant contributions. However, we can extract a charge transfer time for the CF₃-Az₃ SAM by comparing the intensity of the main participator line for the three different alkyl chain length.

Figure 4b shows the decay spectra of CF₃-Az_{*n*} for $n = 3, 6$ and 10 , respectively, recorded at resonance ($h\nu = 285.25$ eV) after subtraction of the non-resonant photoemission background ($h\nu = 275.0$ eV). Prior to subtraction, the spectra have been aligned at the Au 4*f* level and normalized with respect to the NEXAFS spectrum (Fig. 3b), which was recorded in Auger yield. This procedure yielded identical intensities of the Au 6*sp* band close to E_F in non-resonant and resonant photoemission. Comparable to the C1s XP spectra of Fig. 3b the resonant photoemission spectra in Fig. 4b shift by 400 meV to higher kinetic energy (lower binding energy) with decreasing alkyl chain length ($n = 10$ vs. $n = 3$). The identical shift of XP and autoionization spectra suggests that screening of the one-hole and two-holes-one-electron valence states reached after autoionization (*cf.* Fig. 2) is comparable to screening of the 1s core hole. As already discussed, polarization screening of the excited state is dominated by the substrate's contribution and thus rather insensitive to the charge distribution in the chromophore but less effective for larger distance to the metal surface. To evaluate the charge transfer time spectra in Fig. 4b have been normalized

to equal area. The intensity of the HOMO-2,3 participator line for CF₃-Az3 is by $9 \pm 2\%$ smaller than for the longer alkyl spacers $n = 6$ and 10 (see inset of Fig. 4b). Assuming that the distribution between participator and spectator decay in the azobenzene entity is independent of the spacer and that there is no charge transfer to the substrate for a chain length of $n = 10$, the $9 \pm 2\%$ intensity loss can be attributed to non-resonant decay after charge transfer. Applying the core-hole clock yields a charge transfer-time of $\tau_{CT} = \tau_T/0.09 = 73$ fs ($60 - 94$ fs including error bars).

3.4. Two-photon photoemission spectroscopy

Alternatively to the core-hole clock, the charge-transfer time can be studied directly in the time domain employing two-photon photoemission (2PPE) spectroscopy with ultrashort laser pulses [33, 34]. In 2PPE a pump pulse is used to excite the system, while a subsequent probe pulse traces the excited state dynamics by photoionization and subsequent angle- and energy-resolved photoelectron detection. To suppress direct photoemission the photon energy of each pulse is usually kept below the work function Φ , but their sum is sufficient to ionize the system ($h\nu_1 + h\nu_2 > \Phi$). By varying the time delay between pump and probe pulses we can extract the lifetime of the intermediate state from its transient photoelectron signal. The time resolution of the 2PPE experiment is limited to a few femtoseconds when the lifetime can be extracted from the shift and/or broadening of the intermediate state transient with respect to the cross-correlation trace [35]. Longer lifetimes can be more easily determined from the tail of the intermediate state signal at delays when the pump pulse is over, assuming, *e.g.*, exponential decay rates [36]. A clear drawback of 2PPE with respect to resonant photoemission is the fact that one may simply not resolve the unoccupied molecular states. This insensitivity is usually attributed to the low photon energies used to ionize the system, which hamper the coupling of the photoemitted electron to free photocurrent-carrying final states. However, if applicable, the benefit of time-resolved 2PPE over the core-hole clock is that the former directly probes the optical-excited photoswitch in the absence of a

core hole.

Figure 5a shows a false color plot of a time- and energy-resolved 2PPE spectrum for a H-Az3 SAM. The photoemission signal has been integrated over an angular range of $\pm 2^\circ$ around the surface normal. Spectra recorded with either only the pump or the probe pulse have been subtracted. The 2PPE spectrum is quite typical for molecular adsorbates on metal surfaces [5, 37]. Broad spectral features are overlaid with a significant background. When pump and probe pulses overlap, we find intensity for final state energies between 4.35 and 6.3 eV above E_F (left ordinate). The low-energy threshold marks the work function Φ of the H-Az3 SAM. The high energy cut-off corresponds to initial states cut by the Fermi level and shifted by $(h\nu_1 + h\nu_2)$. The 70-fs temporal width of the photoelectron distribution centered at delay zero reflects the cross-correlation of pump and probe pulses. Besides two-photon absorption we can clearly separate two contributions with finite lifetimes. For positive pump-probe delay the pulse with larger photon energy $h\nu_1 = 4.2$ eV acts as pump pulse, while $h\nu_2 = 2.1$ eV is the probe pulse. Likewise the energy scale on the right ordinate refers to intermediate states excited by ultraviolet and ionized by visible light. For negative delay the role of pump and probe pulses is reverted. The intensity at the low-energy cut-off shows long-lived contributions to both sides of the pump-probe delay. Note that the *static* pump- and probe-only spectra have been subtracted. The intensity tail at negative delay is attributed to hot electrons excited in the gold substrate. At the intermediate state energy of ~ 0.2 eV above E_F the lifetime of excited electrons in gold is about 300 fs [38]. The transient intensity at positive delay cannot stem from hot electrons in the gold substrate, since their lifetime at $E - E_F = 2.3$ eV is only ~ 20 fs. It may thus be attributed to the LUMO of the azobenzene chromophore. However, one often observes intensity at the low-energy cut-off of arguable origin, such as inelastic scattering of photoelectrons with primarily higher energy into final states close above the vacuum level E_{vac} [39], and we therefore refrain from evaluating this contribution further.

The 2PPE intensity at 5.7 eV final state energy extends towards positive

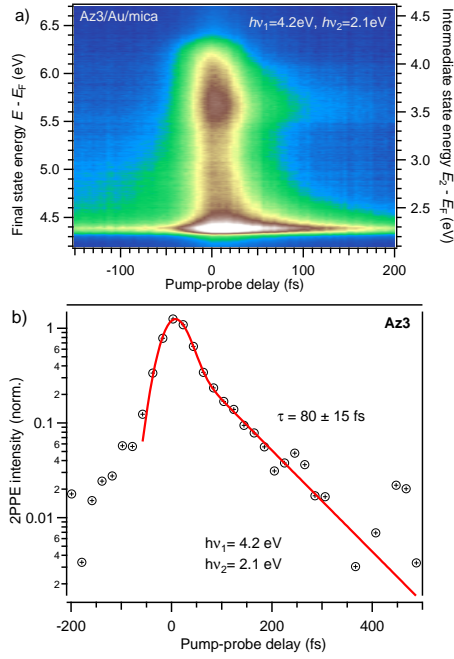


Figure 5: a) False color plot of a time- and energy-resolved 2PPE spectrum for a H-Az3 SAM. The left ordinate refers to the final state energy $E - E_F$. The right ordinate shows the energy of an intermediate state $E_2 - E_F$ populated with the ultraviolet pulse $h\nu_1 = 4.2\text{ eV}$ and ionized with visible light $h\nu_2 = 2.1\text{ eV}$, which refers to positive pump-probe delay. For negative pump-probe delay $h\nu_2$ arrives before $h\nu_1$ at the sample. b) Time-resolved trace extracted in an energy range of $\pm 0.1\text{ eV}$ centered at 3.6-eV intermediate state energy. The solid line is a fit to the data, describing an instantaneous signal plus an exponential decay, both convolved with a 70-fs Gaussian to account for the cross-correlation of pump and probe pulses. The finite lifetime of the intermediate state of $80 \pm 15\text{ fs}$ corresponds to the pure exponential decay seen at delays $> 100\text{ fs}$.

pump-probe delay. It thus stems from an intermediate state at $E_2 - E_F = 3.6$ eV,
270 which is populated by the ultraviolet laser pulse $h\nu_1$ *via* electron transfer from
the gold substrate and ionized by the visible pulse $h\nu_2$. The intermediate state
energy lies 0.1 – 0.2 eV below that of the image-potential state found on pure
alkanethiolate SAMs [40]. Therefore we attribute the transition observed in
the H-Az3 SAM to a negative ion resonance, which couples a LUMO+n of the
275 azobenzene entity to the image-potential state *via* charge transfer and/or hy-
bridization. This may likewise explain, why the pump pulse populates effectively
only one resonance but no lower lying unoccupied molecular orbitals of the chro-
mophore. Our interpretation is in line with a recent 2PPE study of ferrocene
molecules adsorbed on an isolating decanethiolate SAM. For this mixed system
280 Shibuta *et al.* observed only one intermediate state close to the image-potential
state energy, which they likewise attribute to a hybridized molecular resonance
[41].

The lifetime of the molecular resonance was evaluated by integrating the
intensity in an interval of ± 0.1 eV around the peak maximum at 3.6 eV. This
285 yields the time-resolved trace depicted in Fig. 5b in a semi-logarithmic plot.
The solid line is an exponential fit to the data which was convolved with a
Gaussian to account for the cross-correlation of pump and probe pulses. From
the exponential fit we obtain a lifetime of 80 ± 15 fs, which we attribute to the
charge-transfer time between azobenzene photoswitch and gold substrate.

290 3.5. Comparison of charge-transfer times

Applying the core-hole clock, the groups of Menzel, Feulner, and Zharnikov
teamed up to study the charge transfer across alkyl chains varying their length
from two to four CH_2 -groups [15, 16]. They used SAMs with a cyano endgroup
directly coupled to the alkanethiolate and measured the charge-transfer time out
295 of the cyano LUMO after resonant excitation of the $\text{N}1s$ to π^* transition. In the
core-excited state the π^* -LUMO is located at an energy of 0.91 – 0.55 eV above
 E_F for $n = 2 - 4$, respectively. With increasing chain length resonant decay
channels dominate the Auger spectrum and the charge-transfer time from the

cyano endgroup to the substrate increases exponentially with the alkyl chain-
length to $\tau_{CT} = 100 \pm 26$ fs for $n = 4$ [16]. The exponential dependence $\tau_{CT} \propto$
300 $\exp(-\beta d)$ on the barrier thickness d with $\beta = 0.72 \text{ \AA}^{-1}$ [16] can be understood in
a tunnel-barrier or a super-exchange model, which describe the charge transfer
and the related conductivity across the alkyl interface [42, 43].

The charge-transfer time of 100 ± 26 fs for the $n = 4$ alkyl spacer is only
305 slightly larger than $\tau_{CT} = 73_{-13}^{+21}$ fs derived for CF₃-Az3. This suggests that
we can count the oxygen bridge (*cf.* Fig. 1) as an additional spacer unit. It
seems that the charge-transfer time depends primarily on the tunnel-barrier
thickness and is less affected by the variation of the electronic structure along the
chain. This is in line with the observation that the conductivity of SAMs with
310 aromatic spacer units can be described by a β -value of 0.5 \AA^{-1} [44]. Measuring
the conductance of alkanethiols with longer chain lengths ranging from $n = 10$
to 14 through a mercury-drop junction yielded a β parameter of 0.64 \AA^{-1} [43].
This seems close to the value for the short chains, but is likely affected by a
variety of defects that occur within Hg-drop junctions.

315 Applying 2PPE, Shibuta *et al.* studied the charge-transfer time across pure
alkanethiolate SAMs varying the chain-length between $n = 12$ and 18 [40].
Electrons were photoexcited into an image-potential state located in front of the
SAM surface at 3.7 eV above E_F . The charge-transfer time shows a well-defined
exponential increase from about 30 to 80 ps at 90 K [40]. The corresponding
320 β -parameter of 0.097 \AA^{-1} is one order of magnitude smaller than in the above
described experiments. This indicates that β depends strongly on the resonance
position with respect to the barrier heights, which is at $E - E_F \sim 4.0$ eV [45].
In a very recent study the authors used a decanethiolate SAM on Au(111)
as template to adsorb and isolate ferrocene molecules [41]. They observed a
325 molecular hybrid state with a lifetime of 140 fs, which is much shorter than the
image-potential-state lifetime of 11 ps for the pure decanethiolate SAM. This is
in contrast to the larger participator contribution for longer chain length (CF₃-
Az6 and CF₃-Az10), which indicates a significant increase in charge-transfer
time, beyond the sensitivity of the core-hole clock.

330 The charge-transfer time determined by the core-hole clock technique of
73⁺²⁰₋₁₀ fs agrees very well with the lifetime observed in the time-resolved photoemission measurement $\tau_{CT} = 80 \pm 15$ fs. This is surprising since the energetic position of the resonances probed in autoionization and 2PPE are $E - E_F = 1.0$ eV and 3.6 eV and thus significantly different. However, the model of a homogeneous tunneling barrier may be too simple to explain the charge transfer times.
335 Charge transfer out of the strongly localized state probed by resonant core-level excitation generally proceeds faster, as has been observed also for C₆F₆ layers on Cu(111) [46] and has been attributed to a stronger coupling due to broad distribution of parallel momenta in the localized state. In contrast in 2PPE
340 we probe a negative ion resonance which is delocalized in the LUMO+n band of the densely packed SAM. In the case of the CF₃-Az3 SAM this effect seems to be balanced by the lower tunneling barrier for the higher lying resonance probed in 2PPE, since we extract equal charge-transfer times from both techniques. We note that the different endgroups of the azobenzene chromophores
345 (H *vs.* CF₃) should have little effect on the charge transfer time since the probability density of the LUMO+n at the endgroup is negligible (*cf.* Fig. 6 in Ref. [13]). Fully elucidating the dependence of the charge-transfer time on short and long chain lengths and on the energy level alignment will require further 2PPE experiments.

350 The characteristic charge-transfer time is significantly longer than the core-hole lifetime. Therefore charge neutralization occurs long after the photoemission event and the binding energy is lowered by polarization screening of the photo hole. This is corroborated by the shift of the valence states and core levels in the photoemission spectra to higher kinetic energy with decreasing alkyl
355 chain length.

4. Conclusion

Azobenzene-functionalized alkanethiolate SAMs provide a model system to study the dynamics of the deexcitation of photoswitches at a metal surface.

Charge transfer between the azobenzene endgroup and the gold substrate across
360 the alkanthiolate linker of three CH₂ groups and one oxygen bridge occurs on an
ultrafast time scale of ~ 80 fs. The *trans* to *cis* photoisomerization of azobenzene
in solution occurs on a time scale of ~ 1 ps [47, 48, 49]. If charge transfer to
the substrate requires only 100 fs only 10^{-5} of the azobenzene molecules will
remain excited after 1 ps. Compared to azobenzene in solution we observe a five
365 orders of magnitude lower isomerization cross-section in a densely packed H-Az3
SAM at an excitation energy of 3.6 eV corresponding to the $\pi - \pi^*$ transition.
However, increasing the linker length to $n = 11$ CH₂ units and diluting the
molecules with lateral dodecanethiolate spacers switching becomes almost as
effective as in solution [6, 8].

370 5. Acknowledgement

Financial support through Sfb 658 *Elementary processes in molecular switches at surfaces* and through the Helmholtz Virtual Institute *Dynamic Pathways in Multidimensional Landscapes* is gratefully acknowledged.

References

375 References

- [1] N. Katsonis, M. Lubomska, M. M. Pollard, B. L. Feringa, P. Rudolf, Synthetic light-activated molecular switches and motors on surfaces, *Prog. Surf. Sci.* 82 (2007) 407–434.
- [2] R. Klajn, Immobilized azobenzenes for the construction of photoresponsive materials, *Pure Appl. Chem.* 82 (12) (2010) 2247–2279.
- 380 [3] V. Ferri, M. Elbing, G. Pace, M. D. Dickey, M. Zharnikov, P. Samorì, M. Mayor, M. A. Rampi, Light-powered electrical switch based on cargo-lifting azobenzene monolayers, *Angew. Chem., Int. Ed.* 47 (2008) 3407–3409.

- 385 [4] N. Crivillers, E. Orgiu, F. Reinders, M. Mayor, P. Samorì, Optical modulation of the charge injection in an organic field-effect transistor based on photochromic self-assembled-monolayer-functionalized electrodes, *Adv. Mater.* **23** (2011) 1447–1452.
- [5] M. Wolf, P. Tegeder, Reversible molecular switching at a metal surface: A case study of tetra-tert-butyl-azobenzene on Au(111), *Surf. Sci.* **603** (2009) 390 1506–1517.
- [6] C. Gahl, R. Schmidt, D. Brete, E. McNellis, W. Freyer, R. Carley, K. Reuter, M. Weinelt, Structure and excitonic coupling in self-assembled monolayers of azobenzene-functionalized alkanethiols, *J. Am. Chem. Soc.* 395 **132** (2010) 1831–1838.
- [7] B. Baisch, D. Raffa, U. Jung, O. M. Magnussen, C. Nicolas, J. Lacour, J. Kubitschke, R. Herges, Mounting freestanding molecular functions onto surfaces: The platform approach, *J. Am. Chem. Soc.* **131** (2009) 442–443.
- [8] T. Moldt, D. Brete, D. Przyrembel, S. Das, J. R. Goldman, P. K. Kundu, C. Gahl, R. Klajn, M. Weinelt, Tailoring the properties of surface-immobilized azobenzenes by monolayer dilution and surface curvature, *Langmuir* **31** (2015) 1048–1057. 400
- [9] J. C. Love, L. A. Estroff, J. K. Kriebel, R. G. Nuzzo, G. M. Whitesides, Self-assembled monolayers of thiolates on metals as a form of nanotechnology, 405 *Chem. Rev.* **105** (2005) 1103–1169.
- [10] M. Kind, C. Wöll, Organic surfaces exposed by self-assembled organothiol monolayers: Preparation, characterization, and application, *Prog. Surf. Sci.* **84** (2009) 230–278.
- [11] C. Vericat, M. E. Vela, G. Benitez, P. Carro, R. C. Salvarezza, Self-assembled monolayers of thiols and dithiols on gold: new challenges for 410 a well-known system, *Chem. Soc. Rev.* **39** (2010) 1805–1834.

- [12] D. P. Woodruff, The interface structure of n-alkylthiolate self-assembled monolayers on coinage metal surfaces, *Phys. Chem. Chem. Phys.* 10 (2008) 7211–7221.
- 415 [13] R. Schmidt, E. McNellis, W. Freyer, D. Brete, T. Gießel, C. Gahl, K. Reuter, M. Weinelt, Azobenzene-functionalized alkanethiols in self-assembled monolayers on gold, *Appl. Phys. A* 93 (2008) 267–275.
- [14] D. Brete, D. Pryzembel, C. Eickhoff, R. Carley, W. Freyer, K. Reuter, C. Gahl, M. Weinelt, Mixed self-assembled monolayers of azobenzene photo-
420 switches with trifluoromethyl and cyano end-groups, *J. Physics: Cond. mat.* 24 (2012) 394015.
- [15] S. Neppl, U. Bauer, D. Menzel, P. Feulner, A. Shaporenko, M. Zharnikov, P. Kao, D. Allara, Charge transfer dynamics in self-assembled monomolecular films, *Chem. Phys. Lett.* 447 (2007) 227–231.
- 425 [16] P. Kao, S. Neppl, P. Feulner, D. L. Allara, M. Zharnikov, Charge transfer time in alkanethiolate self-assembled monolayers via resonant auger electron spectroscopy, *J. Phys. Chem. C* 114 (2010) 13766–13773.
- [17] W. Freyer, D. Brete, R. Schmidt, C. Gahl, R. Carley, M. Weinelt, Switching
430 behavior and optical absorbance of azobenzene-functionalized alkanethiols in different environments, *J. Photochem. Photobiol. A Chem.* 204 (2009) 102–109.
- [18] P. Feulner, T. Niedermayer, K. Eberle, R. Schneider, D. Menzel, A. Baumer, E. Schmich, A. Shaporenko, Y. Tai, M. Zharnikov, Strong
435 temperature dependence of irradiation effects in organic layers, *Phys. Rev. Lett.* 93 (2004) 178302.
- [19] P. Feulner, T. Niedermayer, K. Eberle, R. Schneider, D. Menzel, A. Baumer, E. Schmich, A. Shaporenko, Y. Tai, M. Zharnikov, Strong
temperature dependence of irradiation effects in organic layers, *Surf. Sci.* 593 (2005) 252–255.

- 440 [20] M. Weinelt, A. Nilsson, M. Magnuson, T. Wiell, O. Karis, M. S. N. Mårtensson, J. Stöhr, Resonant photoemission in Ni metal at the 2p edges: resonant raman and interference effects, *Phys. Rev. Lett.* 78 (1997) 967–970.
- [21] M. P. Seah, Summary of ISO/TC 201, standard VII ISO 15472, 2001 surface
445 chemical analysis x-ray photoelectron spectrometers-calibration of energy scales, *Surf. Interface Anal.* 31 (2001) 721.
- [22] W. Wurth, A. Föhlisch, Electron transfer investigated by x-ray spectroscopy, in: U. Bovensiepen, H. Petek, M. Wolf (Eds.), *Dynamics at Solid State Surfaces and Interfaces*, Vol. 1, Wiley-VCH, Weinheim, 2010, pp.
450 305–322.
- [23] W. Wurth, P. Feulner, D. Menzel, Resonant excitation and decay of adsorbate core holes, *Phys. Scripta.* T41 (1992) 213–216.
- [24] O. Björneholm, A. Sandell, A. Nilsson, N. Mårtensson, J. N. Andersen, Autoionization of adsorbates, *Phys. Scripta.* T41 (1992) 217–225.
- 455 [25] O. Björneholm, A. Nilsson, A. Sandell, B. Herdnäs, N. Mårtensson, Determination of time scales for charge-transfer screening in physisorbed molecules, *Phys. Rev. Lett.* 68 (1992) 1892–1895.
- [26] W. Wurth, G. Rucker, P. Feulner, R. Scheuerer, L. Zhu, D. Menzel, Core excitation and deexcitation in argon multilayers: Surface- and bulk-specific
460 transitions and autoionization versus auger decay, *Phys. Rev. B* 47 (1993) 6697–6704.
- [27] T. X. Carroll, J. Hahne, T. D. Thomas, L. J. Sæthre, N. Berrah, J. Bozek, E. Kukk, Carbon 1s core-hole lifetime in CO₂, *Phys. Rev. A* 61 (2000) 042503.
- 465 [28] N. Saito, A. Hempelmann, F. Heiser, O. Hemmers, K. Wieliczek, J. Viehhaus, U. Becker, Lifetime effects on the dissociation of core-excited n₂ and co molecules, *Phys. Rev. A* 61 (2000) 022709.

- [29] C. L. A. Lamont, J. Wilkes, Attenuation length of electrons in self-assembled monolayers of n-alkanethiols on gold, *Langmuir* 15 (1999) 2037–2042.
- 470
- [30] M. Zharnikov, S. Frey, K. Heister, M. Grunze, An extension of the mean free path approach to x-ray absorption spectroscopy, *J. Elec. Spec. and Rel. Phen.* 124 (2002) 15–24.
- [31] K. Heister, L. S. Johansson, M. Grunze, M. Zharnikov, A detailed analysis of the *c* 1s photoemission of n-alkanethiolate films on noble metal substrates, *Surf. Sci.* 529 (2003) 36–46.
- 475
- [32] D. A. Shirley, High-resolution x-ray photoemission spectrum of the valence bands of gold, *Phys. Rev. B* 5 (1972) 4709–4714.
- [33] H. Petek, S. Ogawa, Femtosecond time-resolved two-photon photoemission studies of electron dynamics in metals, *Prog. Surf. Sci.* 56 (1997) 239–346.
- 480
- [34] M. Weinelt, Time-resolved two-photon photoemission from metal surfaces, *J. Phys.: Condens. Matter* 14 (2002) R1099.
- [35] T. Hertel, E. Knoesel, M. Wolf, G. Ertl, Ultrafast electron dynamics at cu(111): Response of an electron gas to optical excitation, *Phys. Rev. Lett.* 76 (1996) 535–538.
- 485
- [36] I. L. Shumay, U. Höfer, Ch. Reuß, U. Thomann, W. Wallauer, Th. Fauster, Lifetimes of image-potential states on Cu(100) and Ag(100) measured by femtosecond time-resolved two-photon photoemission, *Phys. Rev. B* 58 (1998) 13974–13981.
- [37] S. Hagen, P. Kate, F. Leyssner, D. Nandi, M. Wolf, P. Tegeder, Excitation mechanism in the photoisomerization of a surface-bound azobenzene derivative: Role of the metallic substrate, *J. Chem. Phys.* 129 (2008) 164102.
- 490
- [38] J. Cao, Y. Gao, H. E. Elsayed-Ali, R. J. D. Miller, D. A. Mantell, Femtosecond photoemission study of ultrafast electron dynamics in single-crystal Au(111) films, *Phys. Rev. B* 58 (1998) 10948–10952.
- 495

- [39] S. Hagen, F. Leyssner, D. Nandi, M. Wolf, P. Tegeder, Reversible switching of tetra-tert-butyl-azobenzene on a Au(111) surface induced by light and thermal activation, *Chem. Phys. Lett.* 444 (2007) 85–90.
- [40] M. Shibuta, N. Hirata, R. Matsui, T. Eguchi, A. Nakajima, Charge separation at the molecular monolayer surface: Observation and control of the dynamics, *J. Phys. Chem. Lett.* 3 (2012) 981–985.
- [41] M. Shibuta, N. Hirata, T. Eguchi, A. Nakajima, Probing of an adsorbate-specific excited state on an organic insulating surface by two-photon photoemission spectroscopy, *J. Am. Chem. Soc.* 136 (2014) 1825–1831.
- [42] J. Tomfohr, O. F. Sankey, Theoretical analysis of electron transport through organic molecules, *J. Chem. Phys.* 120 (2004) 1542–1554.
- [43] E. A. Weiss, J. K. Kriebel, M.-A. Rampi, G. M. Whitesides, The study of charge transport through organic thin films: mechanism, tools and applications, *Phil. Trans. R. Soc. A* 365 (2007) 1509–1537.
- [44] B. Kim, J. M. Beebe, Y. Jun, X.-Y. Zhu, C. D. Frisbie, Correlation between homo alignment and contact resistance in molecular junctions: Aromatic thiols versus aromatic isocyanide, *J. Am. Chem. Soc.* 128 (2006) 4970–4971.
- [45] M. Muntwiler, C. D. Lindstrom, X. Y. Zhu, Delocalized electron resonance at the alkanethiolate self-assembled monolayer/Au(111) interface, *J. Chem. Phys.* 124 (2006) 081104.
- [46] A. Föhlisch, S. Vijayalakshmi, A. Pietzsch, M. Nagasono, W. Wurth, P. Kirchmann, P. Loukakos, U. Bovensiepen, M. Wolf, M. Tchapyguine, F. Hennies, Charge transfer dynamics in molecular solids and adsorbates driven by local and non-local excitations, *Surf. Sci.* 606 (2012) 881–885.
- [47] T. Nägele, R. Hoche, W. Zinth, J. Wachtveitl, Femtosecond photoisomerization of cis-azobenzene, *Chem. Phys. Lett.* 272 (1997) 489–495.

- [48] H. Satzger, C. Root, M. Braun, Excited-state dynamics of *trans*- and *cis*-azobenzene after UV excitation in the $\pi\pi^*$ band, J. Phys. Chem. A 108 (2004) 6265–6271.
- 525 [49] I. Conti, M. Garavelli, G. Orlandi, The different photoisomerization efficiency of azobenzene in the lowest $n\pi^*$ and $\pi\pi^*$ singlets: The role of a phantom state, J. Am. Chem. Soc. 130 (2008) 5216–5230.